# Finite element approximation of an unsteady projection-based VMS turbulence model with wall laws

Tomás Chacón Rebollo, Macarena Gómez Mármol, and Samuele Rubino

**Abstract** In this work we present the numerical analysis and study the performance of a finite element projection-based Variational MultiScale (VMS) turbulence model that includes general non-linear wall laws. We introduce Lagrange finite element spaces adapted to approximate the slip condition. The sub-grid effects are modeled by an eddy diffusion term that acts only on a range of small resolved scales. Moreover, high-order stabilization terms are considered, with the double aim to guarantee stability for coarse meshes, and help to counter-balance the accumulation of sub-grid energy together with the sub-grid eddy viscosity term. We prove stability and convergence for solutions that only need to bear the natural minimal regularity, in unsteady regime. We also study the asymptotic energy balance of the system. We finally include some numerical tests to assess the performance of the model described in this work.

## 1 Introduction

This paper deals with the numerical analysis and study of performance of a finite element projection-based VMS model with wall laws in unsteady regime. The projection-based VMS-LES turbulence models (Cf. [20, 21, 22, 23]) are three-level methods with large, sub-filter (resolved) scales and small un-resolved scales. In particular, we will address a multi-scale Smagorinsky modeling of the eddy viscosity, which contains the restriction to the sub-filter scales through a projection/interpolation operator.

T. Chacón-Rebollo and S. Rubino
Dpto. de Ecuaciones Diferenciales y Análisis Numérico & IMUS, Universidad de Sevilla, Spain, e-mail: chacon@us.es, samuele@us.es

M. Gómez-Mármol
Dpto. de Ecuaciones Diferenciales y Análisis Numérico, Universidad de Sevilla, Spain, e-mail: macarena@us.es

The simulation of wall-bounded flows with VMS models may become very expensive in terms of computational resources due to the computation of boundary layers, as this requires very fine meshes in the normal direction to the wall (see, for instance, John and Kindl [25], Bazilevs et al. [3]). A way to overcome this difficulty, recently applied to VMS models, is to weakly impose no-slip boundary conditions (Cf. [4, 5]), that consistently incorporate the "law of the wall" in a weak sense. However, this requires to solve the flow in the whole physical domain (the advantage is the use of uniform meshes vs. stretched meshes, but there is no reduction in number of degrees of freedom). An alternative is the strong imposition of wall laws, which in their turn replace the usual no-slip boundary conditions by modeled conditions that set the stress of the flow at some distance from the wall. This directly permits to avoid the quite costly calculation of the flow near the wall, reducing the computational domain with respect to the physical one (the computational boundary is now inside the physical boundary layer). In this paper, we focus on the combined use of VMS-LES models with general non-linear wall-law boundary conditions (strongly imposed), in the context of the Finite Element Method (FEM).

In particular, we consider a finite element projection-based VMS model that only needs a (fine) grid and interpolation operators on a virtual coarser grid. The large scales are represented in the coarse grid, while the sub-filter scales are their complement into the fine grid. The eddy diffusion term has a projection structure to filter out the large scales and let the eddy diffusion act only on the sub-filter resolved scales. We use high-order term-by-term stabilization to stabilize each single term that could lead to unstable discretizations (e.g. convection, pressure gradient), with high accuracy (Cf. [9, 10, 13]). This allows in particular to use polynomials of the same degree to interpolate velocity and pressure. The used stabilization procedure perfectly fits into the VMS framework. The model includes mixed Dirichlet - wall-law boundary conditions to take into account inflow and solid wall boundaries at the same time.

We perform a numerical analysis of this approximation in unsteady regime (See [12, 33] for the numerical analysis of the steady version of the proposed model). We consider a full space-time discretization, semi-implicit in time. In the framework of this discretization, we prove stability and weak convergence for solutions that only bear the natural minimal regularity: The velocity lies in $L^\infty(\mathbf{L}^2)\cap L^2(\mathbf{H}^1)$ and the pressure in $H^{-1}(L^2)$. This analysis is based upon the representation of the stabilized projection-based VMS discretization as a Galerkin approximation of an augmented weak formulation of the Navier-Stokes equations. This allows to use the standard tools of functional analysis to analyze the stabilized discretization, much as the standard ones for mixed methods. In particular, we estimate in $L^\infty(L^2)$ the primitive in time of the pressure, and we also use Nikolskii space to prove the compactness of the velocity approximation (Cf. Simon [35]). However, the low regularity of the weak solution does not allow to prove the strong convergence of the numerical approximation, and limits the energy balance to an inequality. In particular, we are able to obtain an upper bound for the energy balance, in the case of the Manning wall law (Cf. [28]).

The paper is organized as follows: In Section 2, we present the variational formulation of the continuous and discrete problems we work with, and we state their main properties. Section 3 is devoted to the numerical analysis of the proposed discrete model (stability, convergence) in its unsteady version, and to the study of the asymptotic energy balance of the system. Finally, numerical tests for a fully developed 3D turbulent flow in a channel are presented in Section 4, to assess the performance of the model described in this work.

## 2 The continuous and discrete problems

We introduce a mixed initial-boundary value problem for the incompressible evolution Navier-Stokes equations, which includes a wall-law boundary condition in combination with a Dirichlet boundary condition in the inflow part of the boundary. To avoid unnecessary complexities, we just impose a homogeneous Dirichlet boundary condition, and do not include outflow conditions. General Dirichlet and outflow boundary conditions may be taken into account by standard techniques for Navier-Stokes equations. Let $[0,T]$ be the time interval, and $\Omega$ a bounded polyhedric connected domain in $\mathbb{R}^d$, $d=2$ or 3, with a Lipschitz boundary split into $\Gamma=\overline{\Gamma}_D\cup\overline{\Gamma}_n$. We suppose $\Gamma$ split as the union of the sides $\Sigma_1,\ldots,\Sigma_r$ that we assume to be closed $(d-1)-$dimensional sets (straight segments when $d=2$ or polygons when $d=3$), in such a way that $\overline{\Gamma}_D=\bigcup_{i=1}^{k-1}\Sigma_i$, $\overline{\Gamma}_n=\bigcup_{i=k}^{r}\Sigma_i$, for some integer $k\in\{2,\ldots,r\}$.

We impose a homogeneous Dirichlet inflow boundary condition on $\Gamma_D$ and a wall-law boundary condition on $\Gamma_n$. The problem reads:

*Find* $\mathbf{u}:\Omega\times(0,T)\longrightarrow\mathbb{R}^d$ *and* $p:\Omega\times(0,T)\longrightarrow\mathbb{R}$ *such that:*

$$\left\{\begin{array}{rl}
\partial_t\mathbf{u}+\nabla\cdot(\mathbf{u}\otimes\mathbf{u})-2\nu\nabla\cdot D(\mathbf{u})+\nabla p=\mathbf{f} & \text{in } \Omega\times(0,T),\\
\nabla\cdot\mathbf{u}=0 & \text{in } \Omega\times(0,T),\\
-[\mathbf{n}\cdot 2\nu D(\mathbf{u})]_\tau=\mathbf{g}(\mathbf{u})_\tau & \text{on } \Gamma_n\times(0,T),\\
\mathbf{u}\cdot\mathbf{n}=0 & \text{on } \Gamma_n\times(0,T),\\
\mathbf{u}=\mathbf{0} & \text{on } \Gamma_D\times(0,T),\\
\mathbf{u}(\mathbf{x},0)=\mathbf{u}_0(\mathbf{x}) & \text{in } \Omega,
\end{array}\right. \tag{1}$$

where $\mathbf{u}\otimes\mathbf{u}$ is the tensor function of components $u_iu_j$, $D(\mathbf{u})$ is the symmetric deformation tensor given by $D(\mathbf{u})=(1/2)(\nabla\mathbf{u}+(\nabla\mathbf{u})^t)$, $\mathbf{n}$ is the outer normal to $\Gamma$, the notation $_\tau$ represents the tangential component with respect to $\Gamma$ defined as $\mathbf{u}_\tau=\mathbf{u}-(\mathbf{u}\cdot\mathbf{n})\mathbf{n}$, and $\mathbf{g}:\mathbb{R}^d\to\mathbb{R}^d$ is a given function, which determines the wall law. The unknowns are the velocity $\mathbf{u}$ and the pressure $p$ of the incompressible fluid. The data are the source term $\mathbf{f}$, which represents a body force per mass unit (typically the gravity), the kinematic viscosity $\nu$ of the fluid, which is a positive constant, and the initial data $\mathbf{u}_0$.

*Remark 1.* The analysis performed in the paper strongly uses the assumption that $\Omega$ is a polyhedric domain, to approximate the slip boundary condition $\mathbf{u}\cdot\mathbf{n}=0$ on $\Gamma_n$. There exist well-established techniques to solve this difficulty for domain

with curved boundaries, introduced by Verfürth. For instance, the slip condition may be considered as a restriction, and implemented through a saddle-point problem approach (Cf. [40]). Another possible remedy is to use isoparametric finite elements to fit the curved parts of the boundary (Cf. [39]). We do not consider here this situation, to avoid nonessential complexities that have been treated elsewhere.

## *2.1 Variational formulation of the continuous problem*

We consider the Sobolev spaces $H^s(\Omega)$, $s \in \mathbb{R}$, $L^p(\Omega)$ and $W^{m,p}(\Omega)$, $m \in \mathbb{N}$, $1 \leq p \leq \infty$. We shall use the following notation for vectorial Sobolev spaces: $\mathbf{H}^s$, $\mathbf{L}^p$ and $\mathbf{W}^{m,p}$ respectively shall denote $[H^s(\Omega)]^d$, $[L^p(\Omega)]^d$ and $[W^{m,p}(\Omega)]^d$ (similarly for tensorial spaces of dimension $d \times d$). Also, the parabolic function spaces $L^p(0,T;X)$ and $L^p(0,T;\mathbf{X})$, where $X$ ($\mathbf{X}$) stands for a scalar (vectorial) Sobolev space shall be denoted by $L^p(X)$ and $L^p(\mathbf{X})$, respectively. In order to give a variational formulation of problem (1), let us consider the velocity space $\mathbf{W} = \left\{\mathbf{w} \in \mathbf{H}^1 : \mathbf{w} = \mathbf{0} \text{ on } \Gamma_D, \mathbf{w} \cdot \mathbf{n} = 0 \text{ on } \Gamma_n\right\}$. This is a closed linear subspace of $\mathbf{H}^1$, and thus a Hilbert space endowed with the $\mathbf{H}^1$-norm. Thanks to Korn's inequalities (Cf. [19]), the $\mathbf{H}^1$-norm is equivalent on $\mathbf{W}$ to the norm $\|\mathbf{w}\|_{\mathbf{W}} = \|D(\mathbf{w})\|_{\mathbf{L}^2}$. Also, let us introduce the space of free-divergence functions $\mathbf{W}_{div} = \{\mathbf{w} \in \mathbf{W} : \nabla \cdot \mathbf{w} = 0 \text{ a.e. in } \Omega \times (0,T)\}$. The space $\mathbf{W}_{div}$ is a closed linear subspace of $\mathbf{W}$, and thus a Hilbert space endowed with the $\mathbf{H}^1$-norm. We shall consider the following variational formulation of (1):

*Given* $\mathbf{f} \in L^2(\mathbf{W}')$ *and* $\mathbf{u}_0 \in \mathbf{W}'$, *find* $\mathbf{u} \in L^\infty(\mathbf{L}^2) \cap L^2(\mathbf{W}_{div})$, $P \in L^2(L^2_0)$ *such that:*

$$\begin{cases} -\displaystyle\int_0^T (\mathbf{u}(t), \mathbf{v})_\Omega \varphi'(t)\, dt - \langle \mathbf{u}_0, \mathbf{v} \rangle \varphi(0) \\ \\ +\displaystyle\int_0^T [b(\mathbf{u}(t); \mathbf{u}(t), \mathbf{v}) + a(\mathbf{u}(t), \mathbf{v}) + \langle G(\mathbf{u}(t)), \mathbf{v} \rangle] \varphi(t)\, dt \\ \\ +\displaystyle\int_0^T (P(t), \nabla \cdot \mathbf{v})_\Omega \varphi(t)\, dt = \int_0^T \langle \mathbf{f}(t), \mathbf{v} \rangle \varphi(t)\, dt, \end{cases} \tag{2}$$

for any $\mathbf{v} \in \mathbf{W}$, $\varphi \in \mathscr{D}([0,T])$ such that $\varphi(T) = 0$, where $\langle \cdot, \cdot \rangle$ stands for the duality pairing between $\mathbf{W}$ and its dual $\mathbf{W}'$. The physical pressure is the time derivative of the unknown $P : p = \partial_t P \in H^{-1}(L^2_0) = H^1_0(0,T;L^2_0)'$. The interest of considering $P$ as unknown instead of $p$ is that $P$ naturally belongs to the Banach space $L^\infty(L^2)$. We notice, however, that for practical computations one would approximate the physical pressure $p$, and $P$ is introduced just for the numerical analysis. We shall obtain uniform bounds in this space for its numerical approximations. Also, note that the initial condition takes place in $\mathbf{W}'_{div}$, since $\mathbf{u} \in C^0([0,T], \mathbf{W}'_{div})$ (See [15], Sect. 10.2).

The forms $b$, $a$ and $G$ in (2) are given by:

$$b(\mathbf{w},\mathbf{u},\mathbf{v}) = \frac{1}{2}\left[(\mathbf{w}\cdot\nabla\mathbf{u},\mathbf{v})_\Omega - (\mathbf{w}\cdot\nabla\mathbf{v},\mathbf{u})_\Omega\right], \tag{3}$$

$$a(\mathbf{u},\mathbf{v}) = 2\nu\,(D(\mathbf{u}),D(\mathbf{v}))_\Omega, \tag{4}$$

$$\langle G(\mathbf{u}),\mathbf{v}\rangle = (\mathbf{g}(\mathbf{u}),\mathbf{v})_{\Gamma_n}, \tag{5}$$

for $\mathbf{u}$, $\mathbf{v}$, $\mathbf{w} \in \mathbf{H}^1$. Semicolons $(;)$ are used for form $b$ when it is non-linear with respect to its first argument, i.e. $\mathbf{w} = \mathbf{u}$, as in (2), otherwise comma $(,)$ is used, as in (3). The function $g$ is given in implicit form as:

$$\mathbf{g}(\mathbf{u}) = \begin{cases} \dfrac{\mathbf{u}}{|\mathbf{u}|}(u_\tau)^2 \text{ if } |\mathbf{u}| > 0, \\ \\ \mathbf{0} \qquad\quad \text{if } |\mathbf{u}| = 0, \end{cases}$$

where $u_\tau = u_\tau(|\mathbf{u}|)$ is the wall-friction velocity, computed as unique solution of the algebraic equation:

$$u^+ = L(y^+), \text{ with } u^+ = \frac{|\mathbf{u}|}{u_\tau} \text{ and } y^+ = \frac{u_\tau y}{\nu}. \tag{6}$$

Here, $u^+$ is a friction non-dimensional velocity, $L$ is the wall-law function, obtained from an asymptotic analysis in the boundary layer, $y^+$ denotes a friction non-dimensional normal distance to the solid wall, and $y$ denotes the normal distance to the solid wall. We suppose that the boundary layer is divided into two sub-layers (Cf. [14]):

$$T_1^+ = \Gamma_n \times [0, y_0^+], \quad T_2^+ = \Gamma_n \times [y_0^+, A^+],$$

where $y_0^+$ denotes a fixed friction non-dimensional normal distance to the solid wall. The most common wall-law function is the logarithmic law of Prandtl [32] and Von Kármán [41]:

$$L(y^+) = \begin{cases} y^+ \qquad\qquad\qquad\quad \text{if } y^+ \in [0, y_0^+], \\ \\ \dfrac{1}{C_1}\log(y^+) + C_2 \text{ if } y^+ \in [y_0^+, A^+], \end{cases} \tag{7}$$

where $C_1 \simeq 0.41$ and $C_2 \simeq 5.5$ are constants, calculated from experimental measurements, and $y_0^+$ is chosen by preserving the continuity of $L$ ($y_0^+ \simeq 11.5$). The law (7) does not take into account the transition zone between the viscous and logarithmic sub-layer, called the buffer layer. Actually, there exist other several possible settings of $L$ (e.g., the Spalding's wall law [37]) which model the three boundary sub-layers by a single formula. In all cases, the wall-law function $L$ is non-negative, strictly increasing and continuous, $L'$ admits a finite number of discontinuities, and there exist two positive constants $K_1$ and $K_2$ such that:

$$\lim_{z^+\to 0^+} \frac{L(z^+)}{z^+} = K_1, \quad \lim_{z^+\to\infty} \frac{L(z^+)}{\log z^+} = K_2. \tag{8}$$

This ensures that the associated mapping $G$ is well defined from $\mathbf{W}$ into its dual (Cf. Parés [31]).

## 2.2 Finite element spaces

This section focuses on the construction of finite element (FE) spaces that approximate the slip condition $\mathbf{u}\cdot\mathbf{n}=0$ on $\Gamma_n$.

Let $\{\mathscr{T}_h\}_{h>0}$ be a family of affine-equivalent and conforming (i.e., without hanging nodes) triangulations of $\overline{\Omega}$, formed by triangles or quadrilaterals ($d=2$), tetrahedra or hexaedra ($d=3$). We shall assume that the family of triangulations $\{\mathscr{T}_h\}_{h>0}$ is also admissible in the following sense:

**Definition 1.** The family of triangulations $\{\mathscr{T}_h\}_{h>0}$ is admissible if $\overline{\Gamma}_D$ and $\overline{\Gamma}_n$ are the union of whole sides of elements of $\mathscr{T}_h$.

Given an integer $l\geq 0$, and an element $K\in\mathscr{T}_h$, denote by $\mathbb{R}_l(K)$ either $\mathbb{P}_l(K)$ (i.e., the space of Lagrange polynomials of degree $\leq l$, defined on $K$), if the grids are formed by triangles ($d=2$) or tetrahedra ($d=3$), or $\mathbb{Q}_l(K)$ (i.e., the space of Lagrange polynomials of degree $\leq l$ on each variable, defined on $K$), if the family of triangulations is formed by quadrilaterals ($d=2$) or hexaedra ($d=3$). We consider the following FE spaces for the velocity:

$$\begin{cases} Y_h^l = V_h^l(\Omega) = \{v_h\in C^0(\overline{\Omega}) : v_{h|_K}\in\mathbb{R}_l(K),\forall K\in\mathscr{T}_h\},\\ \\ \mathbf{Y}_h^l = [Y_h^l]^d = \{\mathbf{v}_h\in[C^0(\overline{\Omega})]^d : \mathbf{v}_{h|_K}\in[\mathbb{R}_l(K)]^d,\forall K\in\mathscr{T}_h\},\\ \\ \mathbf{X}_h = \{\mathbf{v}_h\in\mathbf{Y}_h^l : \mathbf{v}_h=\mathbf{0}\text{ on }\overline{\Gamma}_D, \mathbf{v}_h\cdot\mathbf{n}_i=0\text{ on }\Sigma_i, i=k,\ldots,r\}\subset\mathbf{Y}_h^l, \end{cases} \tag{9}$$

where $\mathbf{n}_i$ is the outer normal to $\Sigma_i$ for $i=k,\ldots,r$, and we recall that $\overline{\Gamma}_n=\bigcup_{i=k}^r\Sigma_i$. Hereafter, $\mathbf{Y}_h^l$ (resp., $Y_h^l$) will constitute the discrete foreground vectorial (resp., scalar) spaces in which we will work on.

We prove that the family of spaces $\{\mathbf{X}_h\}_{h>0}$ is effectively an internal approximation of $\mathbf{W}$, i.e. a family of finite-dimensional sub-spaces of $\mathbf{W}$ such that for any $\mathbf{v}\in\mathbf{W}$, $\lim\limits_{h\to 0}\inf\limits_{\mathbf{v}_h\in\mathbf{X}_h}\|\mathbf{v}-\mathbf{v}_h\|_{\mathbf{H}^1}=0$. To do it, let us consider the uniformly stable and convergent Bernardi-Maday-Rapetti (BMR, [6]) interpolation operator $\mathbf{P}_h$ from $\mathbf{H}^1$ on $\mathbf{Y}_h^l$ as follows. Let us denote by $\mathscr{A}_h$ the set of Lagrange interpolation nodes for space $\mathbf{Y}_h^l$. Then:

$$\mathbf{P}_h\mathbf{v}=\sum_{\alpha\in\mathscr{A}_h}\overline{\mathbf{v}}_\alpha\,\lambda_\alpha(\mathbf{x})\quad\text{for }\mathbf{x}\in\overline{\Omega}, \tag{10}$$

where $\lambda_\alpha$ are the canonic basis functions of the Lagrange interpolation, given by:

$$\lambda_\alpha\in Y_h^l,\quad \lambda_\alpha(\beta)=\delta_{\alpha,\beta}\quad\text{for all }\alpha,\beta\in\mathscr{A}_h,$$

with $\delta_{\alpha,\beta}$ the Kronecker delta and $\overline{\mathbf{v}}_\alpha$ an averaged value of $\mathbf{v}$ in a neighborhood of node $\alpha$. Following Chacón and Lewandowski [15], Sect. A.3, it may be proved that if the family of triangulations is admissible, then the values $\overline{\mathbf{v}}_\alpha$ may be chosen to preserve both the no-slip and slip boundary conditions: If $\mathbf{v} \in \mathbf{W}$, then

$$\begin{cases} \overline{\mathbf{v}}_\alpha \cdot \mathbf{n}_{|_F} = 0 & \text{for any } F \in \partial\mathscr{T}_h(\alpha) \text{ if } \alpha \in \mathscr{A}_h \cap \overline{\Gamma}_n, \\ \overline{\mathbf{v}}_\alpha = \mathbf{0} & \text{if } \alpha \in \mathscr{A}_h \cap \overline{\Gamma}_D, \end{cases}$$

where $\partial\mathscr{T}_h(\alpha) = \{F \subset \Gamma \,:\, F \text{ is a side of some element of } \mathscr{T}_h \text{ such that } \alpha \in F\}$, and $\mathbf{n}_{|_F}$ denotes the outer normal to $\Omega$ on $F$. This permits to prove the following:

**Lemma 1.** *Assume that the family of triangulations $\{\mathscr{T}_h\}_{h>0}$ is admissible. Then, $\mathbf{P}_h\mathbf{v} \in \mathbf{X}_h$ if $\mathbf{v} \in \mathbf{W}$.*

The proof of this Lemma can be found in [15] (Sect. 9.3.2), so that we omit it for brevity. Lemma 1 and the convergence in $H^1(\Omega)$ of the BMR interpolation operator $\mathbf{P}_h$ permits easily to conclude that the family $\{\mathbf{X}_h\}_{h>0}$ is an internal approximation of $\mathbf{W}$ for regular triangulations.

## *2.3 A projection-based VMS turbulence model*

We approximate the weak formulation (2) of the initial-boundary value problem (1) for the incompressible evolution Navier-Stokes equations by a projection-based eddy viscosity multi-scale model. To state it, let us introduce the space:

$$\overline{\mathbf{X}}_h = \{\mathbf{v}_h \in \mathbf{Y}_h^{l-1} : \mathbf{v}_h = \mathbf{0} \text{ on } \overline{\Gamma}_D, \mathbf{v}_h \cdot \mathbf{n}_i = 0 \text{ on } \Sigma_i, i = k, \ldots, r\}, \tag{11}$$

and consider a uniformly stable (in $H^1(\Omega)$-norm) interpolation operator $\Pi_h$ on $\overline{\mathbf{Y}}_h$, where:

$$\overline{\mathbf{Y}}_h = [V_h^{l-1}(\Omega)]^d, \tag{12}$$

or:

$$\overline{\mathbf{Y}}_h = [V_H^{l}(\Omega)]^d, \tag{13}$$

and $V_H^l(\Omega)$ in (13) is a sub-space of $V_h^l(\Omega)$ with larger grid size $H > h$ (typically, $H = 2h$ or $H = 3h$). The considered interpolation operator $\Pi_h$ must satisfy optimal error estimates (Cf. [6]), and preserve both the no-slip and slip boundary conditions when restricted to $\mathbf{X}_h$. Thus, we define $\mathbf{X}_h' = (Id - \Pi_h)\mathbf{X}_h$, where $Id$ is the identity operator. In accordance to (12), we identify $\overline{\mathbf{X}}_h = \Pi_h\mathbf{X}_h \subset \overline{\mathbf{Y}}_h = [V_h^{l-1}(\Omega)]^d$ as the large scales velocity space, and $\mathbf{X}_h'$ as the sub-filter scales velocity space. Space $\mathbf{X}_h'$ does not need to be explicitly constructed, only the operator $\Pi_h$ is needed. In accordance to (13), another possible definition of $\overline{\mathbf{X}}_h$ is:

$$\overline{\mathbf{X}}_h = \{\mathbf{v}_h \in [V_H^l(\Omega)]^d : \mathbf{v}_h = \mathbf{0} \text{ on } \overline{\Gamma}_D, \mathbf{v}_h \cdot \mathbf{n}_i = 0 \text{ on } \Sigma_i, i = k, \ldots, r\}. \tag{14}$$

In practical implementations, we consider a standard nodal Lagrange interpolation operator $\Pi_h$ for its simplicity and its efficiency with respect to other choices. This provides quite stable and accurate results. However, there exist other possibilities: we may mention the Scott-Zhang interpolation operator (Cf. [34]), or the already cited BMR (Cf. [6]). Also, the $L^2$-projection is used by John in [24] to define the large scales.

To state the unsteady projection-VMS discretization of (2), consider a positive integer number $N$ and define $\Delta t = T/N$, $t_n = n\Delta t$, $n = 0,1,\ldots,N$. We compute the approximations $\mathbf{u}_h^n$, $p_h^n$ to $\mathbf{u}(\cdot,t_n)$ and $p(\cdot,t_n)$ by:

- **Initialization.** Set:
$$\mathbf{u}_h^0 = \mathbf{u}_{0h}.$$
- **Iteration.** For $n = 0,1,\ldots,N-1$:
*Given* $\mathbf{u}_h^n \in \mathbf{X}_h$, *find* $(\mathbf{u}_h^{n+1}, p_h^{n+1}) \in \mathbf{X}_h \times \mathbb{M}_h$ *such that:*

$$\begin{cases} \left(\dfrac{\mathbf{u}_h^{n+1}-\mathbf{u}_h^n}{\Delta t}, \mathbf{v}_h\right)_\Omega + b(\mathbf{u}_h^n, \mathbf{u}_h^{n+1}, \mathbf{v}_h) + a(\mathbf{u}_h^{n+1}, \mathbf{v}_h) + c'(\mathbf{u}_h^{n+1}; \mathbf{u}_h^{n+1}, \mathbf{v}_h) \\ +\langle G(\mathbf{u}_h^{n+1}), \mathbf{v}_h\rangle - (p_h^{n+1}, \nabla\cdot\mathbf{v}_h)_\Omega + s_{conv}(\mathbf{u}_h^n, \mathbf{u}_h^{n+1}, \mathbf{v}_h) = \langle \mathbf{f}^{n+1}, \mathbf{v}_h\rangle, \\ \\ (\nabla\cdot\mathbf{u}_h^{n+1}, q_h)_\Omega + s_{pres}(p_h^{n+1}, q_h) = 0, \end{cases} \tag{15}$$

for any $(\mathbf{v}_h, q_h) \in \mathbf{X}_h \times \mathbb{M}_h$, where $\mathbb{M}_h = Y_h^l \cap L_0^2(\Omega)$, $\mathbf{f}^{n+1}$ is the average value of $\mathbf{f}$ in $[t_n, t_{n+1}]$, and $\mathbf{u}_{0h}$ is some approximation to $\mathbf{u}_0$ belonging to $\mathbf{X}_h$ (e.g., the discrete $\mathbf{L}^2$-Riesz projection on $\mathbf{X}_h$).

The form $c'$ in (15) provides a multi-scale Smagorinsky modeling of the eddy viscosity (Cf. [36, 11]), given by:

$$c'(\mathbf{u}_h; \mathbf{u}_h, \mathbf{v}_h) = 2(\nu_T(\mathbf{u}_h')D(\mathbf{u}_h'), D(\mathbf{v}_h'))_\Omega, \tag{16}$$

where:

$$\mathbf{u}_h' = \Pi_h^*\mathbf{u}_h, \quad \mathbf{v}_h' = \Pi_h^*\mathbf{v}_h, \quad \Pi_h^* = Id - \Pi_h,$$

and the eddy viscosity $\nu_T$ is defined as:

$$\nu_T(\mathbf{v})(\mathbf{x}) = (C_S h_K)^2 |D(\mathbf{v}_{|_K})(\mathbf{x})| \quad \text{for } \mathbf{x} \in K, \tag{17}$$

where $|\cdot|$ denotes the Frobenius norm on $\mathbb{R}^{d\times d}$ and $C_S$ is a (theoretically) universal constant. However, in practical applications, depending on the flow, the value of $C_S$ may vary between 0.065 (Cf. [29]) and 0.25 (Cf. [26]). Here, we shall use an intermediate value $C_S = 0.1$. The forms $s_{conv}$ and $s_{pres}$ in (15) correspond to a high-order term-by-term stabilized method (Cf. [9, 10, 13]), and are given by:

$$s_{conv}(\mathbf{u}_h; \mathbf{u}_h, \mathbf{v}_h) = \sum_{K\in\mathcal{T}_h} \tau_{v,K}(\sigma_h^*(\mathbf{u}_h\cdot\nabla\mathbf{u}_h), \sigma_h^*(\mathbf{u}_h\cdot\nabla\mathbf{v}_h))_K,$$

$$s_{pres}(p_h, q_h) = \sum_{K \in \mathscr{T}_h} \tau_{p,K}(\sigma_h^*(\nabla p_h), \sigma_h^*(\nabla q_h))_K.$$

Here, $\tau_{v,K}$ and $\tau_{p,K}$ are stabilization coefficients for convection and pressure gradient, respectively, and $\sigma_h^* = Id - \sigma_h$, where $\sigma_h$ is some locally stable (in $L^2(\Omega)$-norm) projection or interpolation operator on the foreground vectorial space $\mathbf{Y}_h^{l-1}$ (also called "buffer space" in this context), satisfying optimal error estimates. In practical implementations, we choose $\sigma_h$ as a Scott-Zhang-like linear interpolation operator on space $\mathbf{Y}_h^{l-1}$ (Cf. [34]). This gives rise to a discretization with a reduced computational cost, but that maintains the same high-order accuracy with respect to standard projection-stabilized methods. For the subsequent numerical analysis, we need the following technical hypothesis on the stabilization coefficients:

**Hypothesis 1** *The stabilization coefficients $\tau_{p,K}$ and $\tau_{v,K}$ satisfy the following condition:*

$$\alpha_1 h_K^2 \leq \tau_{p,K}, \tau_{v,K} \leq \alpha_2 h_K^2, \quad \forall K \in \mathscr{T}_h, \tag{18}$$

*for some positive constants $\alpha_1$ and $\alpha_2$, independent of $h$.*

We work with the following expression for the stabilization coefficients:

$$\tau_{p,K} = \tau_{v,K} = \left\{ \left[ c_1 \frac{\nu + \overline{\nu}_{T|_K}}{(h_K/l)^2} \right] + \left[ c_2 \frac{U_K}{(h_K/l)} \right] \right\}^{-1}, \tag{19}$$

by adapting the form of Codina (Cf. [17]). In (19), $c_1$ and $c_2$ are experimental positive constants, $\overline{\nu}_{T|_K}$ is some local eddy viscosity on element $K$, and $U_K$ is some local speed on element $K$. We assume $U_K$ and $\overline{\nu}_{T|_K}$ positive and uniformly bounded from below and from above, for technical reasons. This ensures (18), in particular.

*Remark 2.* The chosen discretization in time gives rise to a semi-implicit Euler scheme, since the discretization of the convection terms is semi-implicit, while that of the remaining terms is implicit. Note that scheme (15) consists of a high-order discretization method in space (optimal for smooth solutions, Cf. [1, 12, 33]) although, for the sake of simplicity, we shall only consider a first-order discretization in time to perform the numerical analysis. This allows to achieve the stability of the scheme in $L^\infty(\mathbf{L}^2) \cap L^2(\mathbf{H}^1)$ for the velocities. These stability properties are also shared by more general $\theta$-schemes (e.g., Crank-Nicolson scheme). Note that considering the discretization of the convection terms semi-implicit permits to obtain optimal error estimates for rather general fluid viscosities (Cf. [1, 15]), and not just for relatively high viscosities, which is the case for a fully implicit discretization, as well as for the steady version of the model (Cf. [12, 33]).

## 3 Analysis of the discrete model

In this section, we perform the numerical analysis of the proposed unsteady model (15), which we will call in the sequel VMS-S model. For technical reasons, we

assume throughout the work that the family of triangulations $\{\mathscr{T}_h\}_{h>0}$ is uniformly regular. Actually, this technical hypothesis may be relaxed to the more general case of regular grids, but we keep it to focus the analysis on the new aspects of the method, and to not unnecessarily lengthen it.

### *3.1 Technical background*

We state in this subsection some technical results that are required for the numerical analysis. We shall denote throughout the paper by $C$ a constant that may vary from a line to another, but which is always independent of $h$ and $\Delta t$. The analysis is based upon the representation of the stabilizing terms on bubble FE spaces by means of the static condensation operators introduced in Chacón [8].

**Definition 2.** A FE space $\mathbb{Z}_h$, constructed on a triangulation $\mathscr{T}_h$, is called a bubble FE space if, for all $b_h \in \mathbb{Z}_h$, for all $K \in \mathscr{T}_h$, $b_h \in H_0^1(K)$.

A similar definition applies for vectorial bubble FE spaces $\mathbf{Z}_h$.

**Lemma 2.** *There exists a family $\{\mathbf{Z}_h\}_{h>0}$ of bubble FE sub-spaces of $\mathbf{H}_0^1$ and a family $\{S_h\}_{h>0}$ of bilinear uniformly continuous and uniformly coercive forms on $\mathbf{H}_0^1$ such that:*

$$s_{conv}(\mathbf{u}_h;\mathbf{u}_h,\mathbf{v}_h) = S_h(\mathbf{c}_h, R_h(\sigma_h^*(\mathbf{u}_h\cdot\nabla\mathbf{v}_h))), \quad \forall \mathbf{v}_h \in \mathbf{X}_h, \tag{20}$$

$$s_{pres}(p_h,q_h) = S_h(\mathbf{d}_h, R_h(\sigma_h^*(\nabla q_h))), \quad \forall q_h \in \mathbb{M}_h, \tag{21}$$

*where $\mathbf{c}_h = R_h(\sigma_h^*(\mathbf{u}_h\cdot\nabla\mathbf{u}_h))$, $\mathbf{d}_h = R_h(\sigma_h^*(\nabla p_h))$, and $R_h : \mathbf{H}^{-1} \to \mathbf{Z}_h$ is the "static condensation" operator on $\mathbf{Z}_h$ defined as follows:*

*Given $\varphi \in \mathbf{H}^{-1}$, $R_h(\varphi)$ is the only element of $\mathbf{Z}_h$ that satisfies*

$$S_h(R_h(\varphi), z_h) = \langle \varphi, z_h\rangle, \quad \forall z_h \in \mathbf{Z}_h.$$

This result is proved in [8]. We next state a technical result that shall be used to handle the stabilizing terms (Cf. [10]).

**Lemma 3.** *Let $\{z_h\}$ be a sequence of scalar FE bubble functions. Then, for any $p \in [2,6]$ there exists a constant $C_p > 0$ independent of $h$ such that:*

$$\|z_h\|_{L^p(\Omega)} \le C_p\, h^{\alpha}\, \|z_h\|_{H^1(\Omega)}, \text{ where } \alpha = \frac{3}{p} - \frac{1}{2}.$$

Now, we state a specific discrete inf-sup condition for the stabilized approximation, which is essential for the stability of the proposed method.

**Lemma 4.** *Assume that Hypothesis 1 holds. Then, we have the following inf-sup condition:*

$$\forall q_h \in \mathbb{M}_h, \quad ||q_h||_{L^2(\Omega)} \leq C \left( \sup_{\mathbf{v}_h \in \mathbf{X}_h} \frac{(q_h, \nabla \cdot \mathbf{v}_h)_\Omega}{||D(\mathbf{v}_h)||_{\mathbf{L}^2}} + ||R_h(\sigma_h^*(\nabla q_h))||_{\mathbf{H}^1} \right), \quad (22)$$

*for some positive constant C independent of h.*

The proof of this Lemma can be derived from [9]. Note that the discrete inf-sup condition (22) can be extended to a more complex condition that holds for a regular family of triangulations.

Our analysis also needs some properties of the eddy viscosity $\nu_T$ and the form $c'$ (Cf. [12, 15]):

**Lemma 5.** *There exists a constant $C > 0$ only depending on d, $\Omega$ and the aspect ratio of the family of triangulations $\{\mathscr{T}_h\}_{h>0}$ such that:*

$$\|\nu_T(\mathbf{v}_h')\|_{L^\infty(\Omega)} \leq C h^{2-d/2} \|D(\mathbf{v}_h)\|_{\mathbf{L}^2}, \quad (23)$$

$$|c'(\mathbf{v}_h; \mathbf{v}_h, \mathbf{w}_h)| \leq C h^{2-d/2} \|D(\mathbf{v}_h)\|_{\mathbf{L}^2}^2 \|D(\mathbf{w}_h)\|_{\mathbf{L}^2}, \quad (24)$$

*where the aspect ratio of the family of triangulations is defined as the smallest possible constant $\widehat{C}$ such that $h_K \leq \widehat{C}\rho_K$, for any $K \in \mathscr{T}_h$, $h > 0$, and $\rho_K$ is the diameter of the ball inscribed in K.*

We report now the properties of the mapping $G$ that sets the wall-law boundary condition in the Navier-Stokes equations (2) (Cf. [31]):

**Lemma 6.** *The functional G given by (5) is well defined from* $\mathbf{W}$ *into its dual, is monotone, compact, and satisfies the estimates: $\forall \mathbf{v}, \mathbf{w} \in \mathbf{W}$,*

$$\|G(\mathbf{v})\|_{\mathbf{W}'} \leq C(1 + \|\mathbf{v}\|_{\mathbf{H}^1}^2), \quad (25)$$

$$\|G(\mathbf{v}) - G(\mathbf{w})\|_{\mathbf{W}'} \leq C(1 + \|\mathbf{v}\|_{\mathbf{H}^1} + \|\mathbf{w}\|_{\mathbf{H}^1}) \|\mathbf{v} - \mathbf{w}\|_{\mathbf{H}^1}, \quad (26)$$

*where C is a positive constant only depending on d, $\Omega$ and $\Gamma_n$.*

Finally, for the analysis of the unsteady problem (15) we shall use a compactness result on Nikolskii spaces stated in Simon [35].

**Definition 3.** Let $B$ a Banach space. The Nikolskii space of order $r \in [0,1]$ and exponent $p \in [0, +\infty]$ associated with $B$ and a time interval $(0,T)$ is defined as:

$$N^{r,p}(0,T;B) = \{f \in L^p(0,T;B) \text{ such that } \|f\|_{\widehat{N}^{r,p}} < +\infty\},$$

with:

$$\|f\|_{\widehat{N}^{r,p}} = \sup_{\delta > 0} \frac{1}{\delta^r} \|\tau_\delta f\|_{L^p(0,T-\delta;B)},$$

where $\tau_\delta f(t) = f(t+\delta) - f(t)$, $0 \leq t \leq T - \delta$.

Space $N^{r,p}(0,T;B)$, endowed with the norm:

$$\|f\|_{N^{r,p}(0,T;B)} = \|f\|_{L^p(0,T;B)} + \|f\|_{\widehat{N}^{r,p}},$$

is a Banach space. Simon's theorem is stated as follows (Cf. [35]):

**Lemma 7.** *Let $E,F,G$ be Banach spaces such that $E \hookrightarrow F \hookrightarrow G$, where the injection $E \hookrightarrow F$ is compact. Then the injection:*

$$L^p(0,T;E) \cap N^{r,p}(0,T;G) \hookrightarrow L^p(0,T;F) \text{ with } 0 < r < 1,\ 1 \leq p \leq +\infty,$$

*holds and is compact.*

## *3.2 Existence and stability results*

Let us now prove the existence, uniqueness of solution and stability of method (15). To state these results, we shall consider the following discrete functions:

- $\mathbf{u}_h$ is the piecewise linear in time function with values on $\mathbf{X}_h$ such that $\mathbf{u}_h(t_n) = \mathbf{u}_h^n$.
- $\mathbf{c}_h$ and $\mathbf{d}_h$ are the piecewise linear in time functions with values on $\mathbf{Z}_h$ such that $\mathbf{c}_h(t_{n+1}) = \mathbf{c}_h^{n+1} = R_h(\sigma_h^*(\mathbf{u}_h^n \cdot \nabla \mathbf{u}_h^{n+1}))$ and $\mathbf{d}_h(t_{n+1}) = \mathbf{d}_h^{n+1} = R_h(\sigma_h^*(\nabla p_h^{n+1}))$.
- $\widetilde{\mathbf{u}}_h$ is the piecewise constant in time function that takes the value $\mathbf{u}_h^{n+1}$ on $(t_n, t_{n+1})$, and $\mathbf{u}_h(t) = \mathbf{u}_h^0$ in $(-\Delta t, 0)$.
- $\widetilde{\mathbf{u}}_h^-$ is the piecewise constant in time function that takes the value $\mathbf{u}_h^n$ on $(t_n, t_{n+1})$.
- $\widetilde{p}_h$ is the piecewise constant in time function that takes the value $p_h^{n+1}$ on $(t_n, t_{n+1})$.
- $P_h(t) = \displaystyle\int_0^t \widetilde{p}_h(s)\, ds$.

For simplicity of notation, we do not make explicit the dependence of these functions upon $\Delta t$.

**Theorem 2.** *Assume that Hypothesis 1 holds, and let $\mathbf{f} \in L^2(\mathbf{W}')$, $\mathbf{u}_0 \in \mathbf{W}'$. Then, problem (15) admits a unique solution that satisfies the estimates:*

$$\|\mathbf{u}_h\|_{L^\infty(\mathbf{L}^2)} + \sqrt{\nu}\,\|\mathbf{u}_h\|_{L^2(\mathbf{H}^1)} + h_{\min}\,\|D(\mathbf{u}_h')\|_{L^3(\mathbf{L}^3)}^{3/2} + \int_0^T < G(\widetilde{\mathbf{u}}_h(t), \widetilde{\mathbf{u}}_h(t) > dt$$
$$+\sqrt{\nu_S}\left(\|\mathbf{c}_h\|_{L^2(\mathbf{H}^1)} + \|\mathbf{d}_h\|_{L^2(\mathbf{H}^1)}\right) \leq C\left(\|\mathbf{u}_0\|_{\mathbf{W}'} + \frac{1}{\sqrt{\nu}}\|\mathbf{f}\|_{L^2(\mathbf{W}')}\right), \tag{27}$$

$$\|\mathbf{u}_h\|_{N^{1/4,2}(\mathbf{L}^2)} \leq C, \tag{28}$$
$$\|P_h\|_{L^\infty(L^2)} \leq C, \tag{29}$$

*for some constant $C > 0$ independent of $h$ and $\Delta t$, where $h_{\min} = \min\limits_{K \in \mathscr{T}_h} h_K$, and $\nu_S$ is the uniform coerciveness constant of forms $S_h$.*

*Proof.* We proceed by steps.

**Step 1: Existence of solution of discrete problem.** Problem (15) can be written as: *Find $(\mathbf{u}_h^{n+1}, p_h^{n+1}) \in \mathbf{X}_h \times \mathbb{M}_h$ such that*

$$\begin{cases} b(\mathbf{u}_h^n,\mathbf{u}_h^{n+1},\mathbf{v}_h)+\widetilde{a}(\mathbf{u}_h^{n+1},\mathbf{v}_h)+c'(\mathbf{u}_h^{n+1};\mathbf{u}_h^{n+1},\mathbf{v}_h) - (p_h^{n+1},\nabla\cdot\mathbf{v}_h)_\Omega \\ \qquad +\langle G(\mathbf{u}_h^{n+1}),\mathbf{v}_h\rangle + s_{conv}(\mathbf{u}_h^n,\mathbf{u}_h^{n+1},\mathbf{v}_h) = \langle\widetilde{\mathbf{f}}^{n+1},\mathbf{v}_h\rangle, \\ \qquad (\nabla\cdot\mathbf{u}_h^{n+1},q_h)_\Omega + s_{pres}(p_h^{n+1},q_h) = 0, \end{cases} \tag{30}$$

for any $(\mathbf{v}_h,q_h)\in\mathbf{X}_h\times\mathbb{M}_h$, where $\widetilde{a}(\mathbf{u}_h^{n+1},\mathbf{v}_h)=\Delta t^{-1}(\mathbf{u}_h^{n+1},\mathbf{v}_h)+a(\mathbf{u}_h^{n+1},\mathbf{v}_h)$ and $\widetilde{\mathbf{f}}^{n+1}=\mathbf{f}^{n+1}+\Delta t^{-1}\mathbf{u}_h^n$. This problem fits into the same functional framework as the steady VMS-S, since $\widetilde{a}$ is an inner product on space $\mathbf{W}$ that generates a norm equivalent to the $\mathbf{H}^1$-norm. Then, the existence of at least a solution follows from Brouwer's fixed point theorem as for the steady case (Cf. [12, 33]).

**Step 2: Velocity estimates.** To obtain estimate (27), observe that:

$$2(\mathbf{u}_h^{n+1}-\mathbf{u}_h^n,\mathbf{u}_h^{n+1})_\Omega = \|\mathbf{u}_h^{n+1}\|_{\mathbf{L}^2}^2-\|\mathbf{u}_h^n\|_{\mathbf{L}^2}^2+\|\mathbf{u}_h^{n+1}-\mathbf{u}_h^n\|_{\mathbf{L}^2}^2.$$

Then, setting $\mathbf{v}_h=\mathbf{u}_h^{n+1}$ and $q_h=p_h^{n+1}$ in (15), and using Young's inequality, yields:

$$\|\mathbf{u}_h^{n+1}\|_{\mathbf{L}^2}^2+2\Delta t\,\nu\|D(\mathbf{u}_h^{n+1})\|_{\mathbf{L}^2}^2+2\Delta t\,\nu_S\left(\|\mathbf{c}_h^{n+1}\|_{L^2(\mathbf{H}^1)}+\|\mathbf{d}_h^{n+1}\|_{L^2(\mathbf{H}^1)}\right) \tag{31}$$
$$+2\Delta t\,<G(\mathbf{u}_h^{n+1}),\mathbf{u}_h^{n+1}>+2C_S^2h_{\min}^2\Delta t\,\|D(\mathbf{u}_h'^{n+1})\|_{\mathbf{L}^3}^3\le\|\mathbf{u}_h^n\|_{\mathbf{L}^2}^2+\frac{\Delta t}{2\nu}\|\mathbf{f}^{n+1}\|_{\mathbf{W}'}^2.$$

Summing up estimates (31) for $n=0,1,\ldots,k$ for some $k\le N-1$, we obtain:

$$\begin{aligned}&\|\mathbf{u}_h^{k+1}\|_{\mathbf{L}^2}^2+2\Delta t\,\nu\sum_{n=0}^k\|D(\mathbf{u}_h^{n+1})\|_{\mathbf{L}^2}^2+2\Delta t\sum_{n=0}^k<G(\mathbf{u}_h^{n+1}),\mathbf{u}_h^{n+1}>\\&+2\Delta t\,\nu_S\sum_{n=0}^k\left(\|\mathbf{c}_h^{n+1}\|_{L^2(\mathbf{H}^1)}+\|\mathbf{d}_h^{n+1}\|_{L^2(\mathbf{H}^1)}\right)+2C_S^2h_{\min}^2\Delta t\sum_{n=0}^k\|D(\mathbf{u}_h'^{n+1})\|_{\mathbf{L}^3}^3\\&\le\|\mathbf{u}_{0h}\|_{\mathbf{L}^2}^2+\frac{\Delta t}{2\nu}\sum_{n=0}^k\|\mathbf{f}^{n+1}\|_{\mathbf{W}'}^2\le\|\mathbf{u}_0\|_{\mathbf{W}'}^2+\frac{\Delta t}{2\nu}\sum_{n=0}^k\|\mathbf{f}^{n+1}\|_{\mathbf{W}'}^2.\end{aligned} \tag{32}$$

This yields estimate (27), as $\sum_{n=0}^{N-1}\Delta t\,\|\mathbf{f}^{n+1}\|_{\mathbf{W}'}^2\le\|\mathbf{f}\|_{L^2(\mathbf{W}')}^2$, and:

$$\|\mathbf{u}_h\|_{L^\infty(\mathbf{L}^2)}=\max_{n=0,1,\ldots,N}\|\mathbf{u}_h^n\|_{\mathbf{L}^2},\quad \|\mathbf{u}_h\|_{L^2(\mathbf{H}^1)}^2\le C\Delta t\sum_{n=0}^N\|D(\mathbf{u}_h^n)\|_{\mathbf{L}^2}^2,$$

$$\|D(\mathbf{u}_h')\|_{L^3(\mathbf{L}^3)}^3\le C\Delta t\sum_{n=0}^N\|D(\mathbf{u}_h'^n)\|_{\mathbf{L}^3}^3,$$

for some constant $C>0$ independent of $h$ and $\Delta t$.

**Step 3: Uniqueness of solution of discrete problem.** The uniqueness of solutions is a consequence of the well-posedness of the discrete problem (See [15], Sect. 10.7).

**Step 4: Velocity time increment estimates.** Let us write method (15) as:

$$(\partial_t \mathbf{u}_h(t),\mathbf{v}_h)_\Omega + b(\widetilde{\mathbf{u}}_h^-(t);\widetilde{\mathbf{u}}_h(t),\mathbf{v}_h) + a(\widetilde{\mathbf{u}}_h(t),\mathbf{v}_h) + c'(\widetilde{\mathbf{u}}_h(t);\widetilde{\mathbf{u}}_h(t),\mathbf{v}_h) \tag{33}$$
$$+\langle G(\widetilde{\mathbf{u}}_h(t)),\mathbf{v}_h\rangle - (\widetilde{p}_h(t),\nabla\cdot\mathbf{v}_h)_\Omega + S_h\left(\widetilde{\mathbf{c}}_h(t),R_h(\sigma_h^*(\widetilde{\mathbf{u}}_h^-(t)\cdot\nabla\mathbf{v}_h))\right) = \langle\widetilde{\mathbf{f}}_h(t),\mathbf{v}_h\rangle,$$

$$(\nabla\cdot\widetilde{\mathbf{u}}_h(t),q_h)_\Omega + S_h\left(\widetilde{\mathbf{d}}_h(t),R_h(\sigma_h^*(\nabla q_h))\right) = 0, \tag{34}$$

*a.e.*in $[0,T]$, where $\widetilde{\mathbf{c}}_h,\widetilde{\mathbf{d}}_h,\widetilde{\mathbf{f}}_h$ respectively are the piecewise constant functions that take the values $\mathbf{c}_h^{n+1},\mathbf{d}_h^{n+1},\mathbf{f}^{n+1}$ on $(t_n,t_{n+1})$. Integrating (33) in $(t,t+\delta)$ for $t\in[0,T-\delta]$, we have:

$$(\tau_\delta\mathbf{u}_h(t),\mathbf{v}_h)_\Omega = \int_t^{t+\delta}\langle\mathscr{F}_h(s),\mathbf{v}_h\rangle\,ds + \int_t^{t+\delta}(\widetilde{p}_h(s),\nabla\cdot\mathbf{v}_h)_\Omega\,ds, \tag{35}$$

where $\mathscr{F}_h(s)\in\mathbf{W}'$ is given by:

$$\begin{aligned}\langle\mathscr{F}_h(s),\mathbf{v}\rangle \;=\; & -b(\widetilde{\mathbf{u}}_h^-(s);\widetilde{\mathbf{u}}_h(s),\mathbf{v}) - a(\widetilde{\mathbf{u}}_h(s),\mathbf{v}) - c'(\widetilde{\mathbf{u}}_h(s);\widetilde{\mathbf{u}}_h(s),\mathbf{v})\\ & - \langle G(\widetilde{\mathbf{u}}_h(s)),\mathbf{v}\rangle - S_h\left(\widetilde{\mathbf{c}}_h(s),R_h(\sigma_h^*(\widetilde{\mathbf{u}}_h^-(s)\cdot\nabla\mathbf{v}))\right) + \langle\widetilde{\mathbf{f}}_h(s),\mathbf{v}\rangle,\forall\mathbf{v}\in\mathbf{W}.\end{aligned}$$

Setting $\mathbf{v}_h=\tau_\delta\mathbf{u}_h(t)$ in (33) and integrating from 0 to $T-\delta$, we obtain:

$$\begin{aligned}\int_0^{T-\delta}\|\tau_\delta\mathbf{u}_h(t)\|_{\mathbf{L}^2}^2\,dt \;=\; & \int_0^{T-\delta}\int_t^{t+\delta}\langle\mathscr{F}_h(s),\tau_\delta\mathbf{u}_h(t)\rangle\,ds\,dt,\\ & -\int_0^{T-\delta}\int_t^{t+\delta}S_h\left(\tau_\delta\mathbf{d}_h(t),\widetilde{\mathbf{d}}_h(s)\right)ds\,dt := I+II,\end{aligned} \tag{36}$$

where we have used that, from (34):

$$(\nabla\cdot\widetilde{\tau_\delta\mathbf{u}_h}(t),\widetilde{p}_h(s)) = -S_h\left(\widetilde{\tau_\delta\mathbf{d}}_h(t),\widetilde{\mathbf{d}}_h(s)\right).$$

To estimate $I$ in (36), we use in particular the $\mathbf{L}^{4/3}$ stability of the operator $\sigma_h$, which implies:

$$|S_h\left(\widetilde{\mathbf{c}}_h(s),R_h(\sigma_h^*(\widetilde{\mathbf{u}}_h^-(s)\cdot\nabla\mathbf{v}))\right)| \le C\|\widetilde{\mathbf{u}}_h^-(s)\|_{\mathbf{H}^1}\|\widetilde{\mathbf{c}}_h(s)\|_{\mathbf{H}^1}\|\mathbf{v}_h\|_{\mathbf{H}^1}.$$

Then, estimates (24), (26) and the continuity of the forms $b$ and $a$ yield:

$$\begin{aligned}\|\mathscr{F}_h(s)\|_{\mathbf{W}'} \le C\Big[ & \|\widetilde{\mathbf{u}}_h^-(s)\|_{\mathbf{H}^1}^2 + (1+h^{2-d/2})\|D(\widetilde{\mathbf{u}}_h(s))\|_{\mathbf{L}^2}^2 + \|\widetilde{\mathbf{c}}_h\|_{\mathbf{H}^1}^2\\ & +1+\nu\|D(\widetilde{\mathbf{u}}_h(s))\|_{\mathbf{L}^2} + \|\widetilde{\mathbf{f}}_h(s)\|_{\mathbf{W}'}\Big],\end{aligned} \tag{37}$$

where we have used Young's inequality. Due to estimate (27), this implies that the $\mathscr{F}_h$ are uniformly bounded in $L^1(\mathbf{W}')$. Now, using Fubini's theorem:

$$|I| = \left|\int_0^T\int_{s-\delta}^s\langle\mathscr{F}_h(s),\widehat{\tau_\delta\mathbf{u}_h}(t)\rangle\,dt\,ds\right|$$

$$\leq \int_0^T \|\mathscr{F}_h(s)\|_{\mathbf{W}'} \left( \int_{s-\delta}^{s} \|D(\widehat{\tau_\delta \mathbf{u}_h}(t))\|_{\mathbf{L}^2}\, dt \right) ds$$
$$\leq \int_0^T \|\mathscr{F}_h(s)\|_{\mathbf{W}'}\, \delta^{1/2} \left( \int_{s-\delta}^{s} \|D(\widehat{\tau_\delta \mathbf{u}_h}(t))\|_{\mathbf{L}^2}^2\, dt \right)^{1/2} ds$$
$$\leq C\,\delta^{1/2} \|\mathbf{u}_h\|_{L^2(\mathbf{H}^1)} \leq C\,\delta^{1/2}, \tag{38}$$

for some constant $C$ independent of $h$, where $\widehat{\cdot}$ denotes the extension by zero of a function outside $[0, T-\delta]$. The last line above follows from (27) and (37).
The term $II$ in (36) is estimated similarly. We apply Fubini's theorem:

$$|II| = \left| \int_0^T \int_{s-\delta}^{s} S_h \left( \widehat{\tau_\delta \mathbf{d}_h}(t), \mathbf{d}_h(s) \right) dt\, ds \right|$$
$$\leq C \int_0^T \int_{s-\delta}^{s} \|\nabla \widehat{\tau_\delta \mathbf{d}_h}\|_{\mathbf{L}^2} \|\nabla \mathbf{d}_h(s)\|_{\mathbf{L}^2}\, dt\, ds$$
$$\leq C \int_0^T \|\nabla \mathbf{d}_h(s)\|_{\mathbf{L}^2}\, \delta^{1/2} \left( \int_{s-\delta}^{s} \|\nabla \widehat{\tau_\delta \mathbf{d}_h}(t))\|_{\mathbf{L}^2}^2\, dt \right)^{1/2} ds$$
$$\leq C\,\delta^{1/2} \|\mathbf{d}_h\|_{L^1(\mathbf{H}^1)} \|\mathbf{d}_h\|_{L^2(\mathbf{H}^1)} \leq C\,\delta^{1/2}, \tag{39}$$

where we have used the uniform continuity of the forms $S_h$ for pressure, and again the last estimate follows from (27). Consequently, estimate (28) follows.

**Step 5: Estimate of the time primitive of the pressure.** Integrating (33) in time from 0 to $t$, we obtain:

$$(P_h(t), \mathbf{v}_h)_\Omega = (\mathbf{u}_h(t) - \mathbf{u}_{0h}, \mathbf{v}_h)_\Omega - \int_0^t \langle \mathscr{F}_h(s), \mathbf{v}_h \rangle\, ds$$
$$\leq C \left( \|\mathbf{u}_h\|_{L^\infty(\mathbf{L}^2)} + \|\mathbf{u}_{0h}\|_{\mathbf{L}^2} + \|\mathscr{F}\|_{L^1(\mathbf{W}')} \right) \|\mathbf{v}_h\|_{\mathbf{H}^1} \leq C \|\mathbf{v}_h\|_{\mathbf{H}^1},$$

where the last estimate follows from estimates (27) and (37). Also:

$$R_h(\sigma_h^*(\nabla P_h(t))) = \int_0^t R_h(\sigma_h^*(\nabla \widetilde{p}_h(s)))\, ds = \int_0^t \widetilde{\mathbf{d}}_h(s)\, ds.$$

Using again (27), we deduce:

$$\|R_h(\sigma_h^*(\nabla P_h(t)))\|_{\mathbf{H}^1} \leq C \|\mathbf{d}_h\|_{L^1(\mathbf{H}^1)} \leq C.$$

Then, by the inf-sup condition (22), estimate (29) follows. □

*Remark 3.* The estimate (27) for the convective and pressure stabilizing terms guarantees an extra-control on the high frequencies of the convective derivative and pressure gradient, which is not obtained by standard projection-based VMS methods (Cf. [25]), for which only the sub-grid eddy viscosity term of Smagorinsky type is added to the standard Galerkin discretization.

### *3.3 Convergence analysis*

To prove convergence, we need some preliminary results (Cf. [15]).

**Lemma 8.** *Let* $\mathbf{z} \in L^\infty(\mathbf{L}^2) \cap L^2(\mathbf{L}^4)$. *Then,* $\mathbf{z} \in L^3(\mathbf{L}^3)$ *and:*

$$\|\mathbf{z}\|_{L^3(\mathbf{L}^3)} \leq \|\mathbf{z}\|^{1/3}_{L^\infty(\mathbf{L}^2)} \|\mathbf{z}\|^{2/3}_{L^2(\mathbf{L}^4)}. \tag{40}$$

**Lemma 9.** *Assume that the sequence* $\{\widetilde{\mathbf{u}}_h^-\}_{h>0} \subset C^0(\mathbf{W}_h)$ *strongly converges to* $\mathbf{u}$ *in* $L^3(\mathbf{L}^3)$, *and that* $\{\mathbf{v}_h\}_{h>0} \subset \mathbf{X}_h$ *strongly converges to* $\mathbf{v} \in \mathbf{W}$ *in* $\mathbf{W}$. *Let* $\varphi \in \mathscr{D}([0,T])$. *Then* $\widetilde{u}_{ih}^-(\mathbf{x},t)\, v_{jh}(\mathbf{x})\, \varphi(t)$ *strongly converges to* $\widetilde{u}_i(\mathbf{x},t)\, v_j(\mathbf{x})\, \varphi(t)$ *in* $L^2(\mathbf{L}^2)$, $i,j = 1,\ldots,d$, *where we denote* $\widetilde{\mathbf{u}}_h^- = (\widetilde{u}_{1h}^-,\ldots,\widetilde{u}_{dh}^-)$, $\mathbf{v}_h = (v_{1h},\ldots,v_{dh})$.

The convergence of method (15) is now stated as follows:

**Theorem 3.** *Assume that* $\mathbf{f} \in L^2(\mathbf{W}')$, $\mathbf{u}_0 \in \mathbf{L}^2$, *and Hypothesis 1 holds. Then, the sequence* $\{(\mathbf{u}_h, P_h)\}_{h>0}$ *contains a sub-sequence* $\{(\mathbf{u}_{h'}, P_{h'})\}_{h'>0}$ *that is weakly convergent in* $L^2(\mathbf{H}^1) \times L^2(L^2)$ *to a weak solution* $(\mathbf{u}, P)$ *of the unsteady Navier-Stokes equations (2). Moreover,* $\{\mathbf{u}_{h'}\}_{h'>0}$ *is weakly-* convergent in* $L^\infty(\mathbf{L}^2)$ *to* $\mathbf{u}$, *strongly in* $L^2(\mathbf{H}^s)$ *for* $0 \leq s < 1$, *and* $\{P_{h'}\}_{h'>0}$ *is weakly-* convergent in* $L^\infty(L^2)$ *to* $P$. *If the solution of problem (2) is unique, then the whole sequence converges to it.*

*Proof.* We proceed by steps.

**Step 1: Extraction of convergent sub-sequences.** Observe that, if the discrete initial condition is given by the $\mathbf{L}^2$-Riesz projection of $\mathbf{u}_0$ on $\mathbf{X}_h$ (as we are assuming), then $\|\mathbf{u}_{0h}\|_{\mathbf{L}^2} \leq \|\mathbf{u}_0\|_{\mathbf{L}^2}$. Then, the uniform estimates for $\mathbf{u}_h$ in $L^2(\mathbf{H}^1)$ and $N^{1/4,2}(\mathbf{L}^2)$ obtained in Theorem 2 ensure the compactness of the sequence $\{\mathbf{u}_h\}_{h>0}$ in $L^2(\mathbf{H}^s)$, where we have used the compactness result of Lemma 7. Also, by estimate (29), the sequence $\{P_h\}_{h>0}$ is uniformly bounded in $L^\infty(L^2)$. Then, the sequence $\{(\mathbf{u}_h, P_h)\}_{h>0}$ contains a sub-sequence (that we denote in the same way) such that $\{\mathbf{u}_h\}_{h>0}$ is strongly convergent in $L^2(\mathbf{H}^s)$ to some $\mathbf{u}$, weakly in $L^2(\mathbf{H}^1)$, and weakly-* in $L^\infty(\mathbf{L}^2)$, and $\{P_h\}_{h>0}$ is weakly-* convergent in $L^\infty(L^2)$ to some $P$. We give in the sequel a sketch of the proof showing that $(\mathbf{u}, P)$ is a weak solution of (2).

Also, note that by (27) the sequence $\{\widetilde{\mathbf{u}}_h\}_{h>0}$ is uniformly bounded in $L^2(\mathbf{H}^1)$ and in $L^\infty(\mathbf{L}^2)$. Then, it contains a sub-sequence weakly convergent in $L^2(\mathbf{H}^1)$ and weakly-* in $L^\infty(\mathbf{L}^2)$ to some $\mathbf{v}$. Both limit functions $\mathbf{u}$ and $\mathbf{v}$ are equal, since one can prove (Cf. [10, 15]) that $\widetilde{\mathbf{u}}_h$ strongly converges to $\mathbf{u}$ in $L^2(\mathbf{L}^2)$. Observe that similarly $\widetilde{\mathbf{u}}_h^-$ strongly converges in $L^2(\mathbf{L}^2)$ to $\mathbf{u}$.

**Step 2: Limit of the continuity equation.** To pass to the limit in the continuity equation, we consider a test function $q \in \mathscr{D}(\Omega) \cap L^2_0(\Omega)$, and some interpolant $q_h \in \mathbb{M}_h$, strongly convergent to $q$ in $L^2_0(\Omega)$ and satisfying optimal error estimates. Observe that:

$$\begin{aligned}
\|\sigma_h^*(\nabla q_h)\|_{\mathbf{L}^2} &\leq \|\sigma_h^*(\nabla(q_h - q))\|_{\mathbf{L}^2} + \|\sigma_h^*(\nabla q)\|_{\mathbf{L}^2} \\
&\leq C\|\nabla(q_h - q)\|_{\mathbf{L}^2} + \|\sigma_h^*(\nabla q)\|_{\mathbf{L}^2} \\
&\leq C\left(h^m \|q\|_{H^{m+1}(\Omega)} + h^l \|q\|_{H^{l+1}(\Omega)}\right), \text{ for } m,l \geq 1.
\end{aligned}$$

Then, for any $\varphi \in C^\infty([0,T])$:

$$\left|\int_0^T S_h(R_h(\sigma_h^*(\nabla q_h)),\widetilde{\mathbf{d}}_h(t))\varphi(t)\,dt\right| = \left|\int_0^T (\sigma_h^*(\nabla q_h),\widetilde{\mathbf{d}}_h(t))_\Omega\,\varphi(t)\,dt\right|$$
$$\leq C\,h\,\|\varphi\|_{L^\infty(0,T)}\int_0^T \|\widetilde{\mathbf{d}}_h(t)\|_{\mathbf{L}^2}\,dt \to 0,\ \text{as } h\to 0.$$

Consequently, as $\nabla\cdot\widetilde{\mathbf{u}}_h$ weakly converges to $\nabla\cdot\mathbf{u}$ in $L^2(\mathbf{L}^2)$, from (34) we have:

$$\int_0^T (\nabla\cdot\mathbf{u}(t),q)_\Omega\,\varphi(t)\,dt = \lim_{h\to 0}\int_0^T (\nabla\cdot\widetilde{\mathbf{u}}_h(t),q_h)_\Omega\,\varphi(t)\,dt$$
$$= -\lim_{h\to 0}\int_0^T S_h(R_h(\sigma_h^*(\nabla q_h)),\widetilde{\mathbf{d}}_h(t))\varphi(t)\,dt = 0.$$

The same property readily holds for $q=1$, since $\mathbf{u}\in\mathbf{W}$. As the set of functions $\{\phi(x,t)=q(x)\,\varphi(t),\ \text{for } q\in\mathscr{D}(\Omega),\varphi\in\mathscr{D}(0,T)\}$ is dense in $L^2(L^2)$ (Cf. Lions [27]), we deduce that $\nabla\cdot\mathbf{u}=0$ *a.e.* in $\Omega\times(0,T)$.

**Step 3: Limit of the momentum equation.** To pass to the limit in the momentum conservation equation (33), we reformulate it as:

$$-\int_0^T (\mathbf{u}_h(t),\mathbf{v}_h)_\Omega\,\varphi'(t)\,dt - (\mathbf{u}_{0h},\mathbf{v}_h)_\Omega\,\varphi(0) + \int_0^T b(\widetilde{\mathbf{u}}_h^-(t);\widetilde{\mathbf{u}}_h(t),\mathbf{v}_h)\,\varphi(t)\,dt$$
$$+\int_0^T a(\widetilde{\mathbf{u}}_h(t),\mathbf{v}_h)\,\varphi(t)\,dt + \int_0^T c'(\widetilde{\mathbf{u}}_h(t);\widetilde{\mathbf{u}}_h(t),\mathbf{v}_h)\,\varphi(t)\,dt$$
$$+\int_0^T \langle G(\widetilde{\mathbf{u}}_h(t)),\mathbf{v}_h\rangle\,\varphi(t)\,dt + \int_0^T (P_h(t),\nabla\cdot\mathbf{v}_h)_\Omega\,\varphi'(t)\,dt$$
$$+\int_0^T S_h(\widetilde{\mathbf{c}}_h(t),R_h(\sigma_h^*(\widetilde{\mathbf{u}}_h^-(t)\cdot\nabla\mathbf{v}_h)))\varphi(t)\,dt = \int_0^T \langle\widetilde{\mathbf{f}}_h(t),\mathbf{v}_h\rangle\,\varphi(t)\,dt, \tag{41}$$

for any function $\varphi\in\mathscr{D}([0,T])$ such that $\varphi(T)=0$. Let $\mathbf{v}\in\mathbf{W}$ be a test function. As $\mathbf{X}_h$ is an internal approximation of $\mathbf{W}$ (See Subsection 2.2), then there exists a sequence $\{\mathbf{v}_h\}_{h>0}\in\mathbf{X}_h$ strongly convergent to $\mathbf{v}\in\mathbf{W}$. By using Lemma 8 for the time derivative term and Lemma 9 for the convection term, then the proof of the convergence of the standard Galerkin plus the wall-law terms follows by rather standard arguments (See [15], Sect. 10.4 for details). Also, by (24), the multi-scale eddy diffusion term vanishes in the limit. To pass to the limit in the stabilizing term for convection, we write:

$$\left|\int_0^T S_h(\widetilde{\mathbf{c}}_h(t),R_h(\sigma_h^*(\widetilde{\mathbf{u}}_h^-(t)\cdot\nabla\mathbf{v}_h)))\varphi(t)\right| = \left|\int_0^T (\widetilde{\mathbf{c}}_h(t),\sigma_h^*(\widetilde{\mathbf{u}}_h^-(t)\cdot\nabla\mathbf{v}_h))_\Omega\,\varphi(t)\right|$$
$$\leq \|\varphi\|_{L^\infty(0,T)}\int_0^T \|\sigma_h^*(\widetilde{\mathbf{u}}_h^-(t)\cdot\nabla\mathbf{v}_h)\|_{\mathbf{L}^{3/2}}\|\widetilde{\mathbf{c}}_h(t)\|_{\mathbf{L}^3}\,dt$$
$$\leq C\,\|\varphi\|_{L^\infty(0,T)}\int_0^T \|\widetilde{\mathbf{u}}_h^-(t)\|_{\mathbf{L}^6}\|\nabla\mathbf{v}_h\|_{\mathbf{L}^2}\|\widetilde{\mathbf{c}}_h(t)\|_{\mathbf{L}^3}\,dt$$

$$\leq C\|\varphi\|_{L^\infty(0,T)}\|\nabla \mathbf{v}_h\|_{\mathbf{L}^2}\left(\int_0^T \|\widetilde{\mathbf{u}}_h^-(t)\|_{\mathbf{L}^6}^2\,dt\right)^{1/2}\left(\int_0^T \|\widetilde{\mathbf{c}}_h(t)\|_{\mathbf{L}^3}^2\,dt\right)^{1/2}$$
$$\leq C\|\varphi\|_{L^\infty(0,T)}\|\nabla \mathbf{v}_h\|_{\mathbf{L}^2}\|\widetilde{\mathbf{u}}_h^-\|_{L^2(\mathbf{H}^1)}\|\widetilde{\mathbf{c}}\|_{L^2(\mathbf{H}^1)}h^{1/2} \leq C\|\varphi\|_{L^\infty(0,T)}\|\nabla \mathbf{v}_h\|_{\mathbf{L}^2}h^{1/2},$$

where we have used the stability of the interpolation operator $\sigma_h$ in $\mathbf{L}^{3/2}$, the stability estimate (27) and Lemma 3. Thus, by the preceding analysis, we deduce that $(\mathbf{u},P)$ is a weak solution of (2).

**Step 4: Uniqueness.** As the convergence analysis follows from a compactness argument, it is standard to prove, by *reductio ad absurdum*, that if the limit, solution of (2), is unique, then the whole sequence converges to it. □

### *3.4 Asymptotic energy balance*

Due to the low regularity of the weak solution, we are not able to get an asymptotic energy identity. We can prove an energy inequality, related to the dissipative nature of the approximation (15), for some simplified wall laws. Indeed, assume that the wall law is given by the Manning formula (Cf. [28]):

$$\mathbf{g}(\mathbf{u}) = c_f|\mathbf{u}|\mathbf{u},$$

where $c_f$ is a friction coefficient. Then, the following holds:

**Lemma 10.** *Let $\mathbf{u} \in L^\infty(\mathbf{L}^2)\cap L^2(\mathbf{W}_{div})$ be a weak solution [together with some pressure $p \in \mathscr{D}'(\Omega\times(0,T))$] of problem (2), which is obtained as a weak limit of some sequence $\{\mathbf{u}_h\}_{h>0}$ in the terms stated in Theorem 3. Then:*

$$\frac{1}{2}\|\mathbf{u}(t)\|_{\mathbf{L}^2}^2 + 2\nu\int_0^t \|D(\mathbf{u}(s))\|_{\mathbf{L}^2}^2\,ds + \int_0^t\int_{\Gamma_n}\langle G(\mathbf{u}(s)),\mathbf{u}(s)\rangle\,ds \leq \frac{1}{2}\|\mathbf{u}_0\|_{\mathbf{L}^2}^2 + \int_0^t\langle \mathbf{f}(s),\mathbf{u}(s)\rangle\,ds, \quad (42)$$

*for almost every $t\in[0,T]$.*

*Remark 4.* In the proof of (42) (Cf. [15], Sect. 10.6), the sub-grid dissipation energy term so as the sub-grid stabilizing energy terms are treated only using that they are positive. By estimate (27), they are uniformly bounded with respect to $h$ and $\Delta t$. However, stability estimate (27), combined with inverse inequalities, is not sufficient to prove that these terms asymptotically vanishes (further regularity is needed to ensure it).

# 4 Numerical experiments: turbulent channel flow

In this section, we discuss some numerical results to analyze the basic numerical performances of the proposed model applied to the computation of turbulent flows, with and without wall-law boundary conditions. In particular, we present results of a fully developed 3D turbulent flow in a channel at $Re_\tau = 180$ for coarse grids. The turbulent flow in a 3D lid-driven cavity at higher Reynolds numbers up to $Re = 10^4$ was investigated by the third author in [15] and [33] applying the same turbulence model described in the present paper, but just with Dirichlet boundary conditions.

## *4.1 Setting for numerical simulations*

The proposed test consist of a fluid that flows between two parallel walls driven by an imposed pressure gradient source term which is defined by the Reynolds number $Re_\tau$ based on the wall shear velocity $u_\tau$. For the setup of our numerical simulations, we choose to follow the guidelines given by Gravemeier in [18] (See [12, 33] for a detailed description of the setting). As a benchmark, we will use the fine Direct Numerical Simulation (DNS) of Moser, Kim and Mansour [30]. In particular, we test the following different settings of the eddy viscosity term for the proposed turbulence model:

- SMA model: The Smagorinsky setting, given by

$$c'(\mathbf{u}_h;\mathbf{u}_h,\mathbf{v}_h) = 2(\nu_T(\mathbf{u}_h)D(\mathbf{u}_h),D(\mathbf{v}_h))_\Omega;$$

- VMS-S model: The *Small-Small* VMS-Smagorinsky setting, given by

$$c'(\mathbf{u}_h;\mathbf{u}_h,\mathbf{v}_h) = 2(\nu_T(\mathbf{u}'_h)D(\mathbf{u}'_h),D(\mathbf{v}'_h))_\Omega;$$

- VMS-B model: A modified version of Berselli-Iliescu-Layton setting of Ref. [7], in which:

$$c'(\mathbf{u}_h;\mathbf{u}_h,\mathbf{v}_h) = 2(\nu_T(\widetilde{\Pi}_h^* D(\mathbf{u}_h))\widetilde{\Pi}_h^* D(\mathbf{u}_h),\widetilde{\Pi}_h^* D(\mathbf{v}_h))_\Omega,$$

  where $\widetilde{\Pi}_h^* = Id - \widetilde{\Pi}_h$, and we have denoted by $\widetilde{\Pi}_h$ an interpolation operator on a coarser (e.g., $P0$) FE space.

The boundary conditions are periodic in both the stream-wise and span-wise directions (homogeneous directions). We perform a comparison between the application of wall-law and no-slip boundary conditions at the walls.

Our strategy is as follows: to reach a statistically steady state, we use an evolution approach starting by an initial parabolic velocity profile perturbed by a random velocity fluctuation. We first run a simulation with no-slip boundary conditions at the walls, in order to stabilize $u_\tau$ near a unitary value, for which we choose to work with Van Driest damping [38] too.

The difficulty we face in the numerical simulations is to obtain a good accuracy with a relatively coarse spatial resolution. Our grid consists of a $16^3$ partition of the channel, uniform in the homogeneous directions. The distribution of nodes in the wall-normal direction is non-uniform, and obeys the cosine function of Gauss-Lobatto. We use three-dimensional $P2$ FE for velocity and pressure. A simulation equivalent in number of degrees of freedom (d.o.f.) to our discretization for a turbulent channel flow at $Re_\tau = 180$ has been carried out by Akkerman in his PhD thesis [2], by using a residual-based VMS (RB-VMS) turbulence model. Note that this discretization is four times coarser than the DNS one.

We use the Crank-Nicolson scheme for the temporal discretization, combined with linearization of convective and sub-grid eddy viscosity terms. The choice of this modified Crank-Nicolson scheme is due to the fact that it provides a good compromise between accuracy and computational complexity, while keeping the numerical diffusion levels below the sub-grid terms (Cf. [25]). The discretized scheme is first integrated for 1250 time steps, with $\Delta t = 0.004$. This time step is smaller than the Kolmogorov time scale, and it fits into the range proposed in [16] to ensure numerical stability (Cf. [25]). Within this time period, the flow is expected to develop to full extent, including a subsequent relaxation time.

Afterwards, we further integrate in parallel the numerical schemes either with no-slip boundary conditions and wall-law boundary conditions, within another 1250 time steps, in order to collect statistics and perform a comparison. We choose to apply wall-law boundary conditions only to VMS-S method, which is the model that gives the most promising results. We consider the logarithmic wall-law of Prandtl and Von Kármán, where we fix the computational boundary at $y^+ = 11.5$, and we use a uniform mesh with 12 grid-lines in wall-normal direction, neglecting the use of Van Driest damping too. This permits to avoid the quite costly calculation of the flow near the walls, reducing the number of d.o.f., with a saving in computing time of about 34% compared with the use of no-slip boundary conditions. Note that before the flow becomes quasi-stationary, the value of $u_\tau$ changes a lot in time, and this implies a dynamic development of the boundary layer thickness, due to the definition of $y^+$. This requires a dynamic adaptation in the use of wall laws. Here, we choose a simpler procedure, letting the flow develop until reaching a stable configuration before applying wall laws in a static way.

## *4.2 Numerical results*

Hereafter, we denote by $\langle\cdot\rangle$ the mean values and by $\widetilde{\cdot}$ the respective fluctuations, where mean values are obtained averaging over all time steps of the statistical period as well as over the homogeneous directions. In Figure 1, we show the mean streamwise velocity profile $\langle u_1 \rangle$ (first-order statistic), normalized by the computed $u_\tau$, in wall coordinates $y^+$. As usual, only half of the channel width is illustrated (i.e., the upper half-width here).

In particular, the displayed mean stream-wise velocity profiles are obtained by using both no-slip boundary conditions (for all methods) and wall-law boundary conditions (for VMS-S method), and a comparison is performed with DNS data [30] and the numerical results of Akkerman [2]. Note that the DNS data so as the RB-VMS results of Akkerman are obtained by the standard approach that uses no-slip boundary conditions at the walls. The results show an acceptable agreement with the fine DNS, even with the very coarse basic discretization at hand. The profiles obtained with the wall-law boundary conditions starting from $y^+ = 11.5$ are simply extended linearly up to the wall located at $y^+ = 0$. We are entitled to do so, because in this case the leading component of the velocity is the stream-wise velocity, so that we can "identify" the friction non-dimensional velocity $u^+$, defined in (6), by $\langle u_1 \rangle / u_\tau$. We display in Table 1 (first column) the deviation $e_0^{\langle u_1 \rangle}$ for the mean stream-wise velocity profile from the respective DNS data in a normalized discrete $L^2$-norm subject to:

$$e_0^{\langle u_1 \rangle} = \left[ \frac{\displaystyle\int_{y^+=0}^{y^+=180} |\langle u_1 \rangle_h^+ - \langle u_1 \rangle_{DNS}^+|^2 \, dy^+}{\displaystyle\int_{y^+=0}^{y^+=180} |\langle u_1 \rangle_{DNS}^+|^2 \, dy^+} \right]^{1/2} . \tag{43}$$

We can observe as all methods give similar errors levels between 11% and 22%.

**Table 1** $L^2$-norm of the deviation from the DNS profiles for the stream-wise velocity.

| Methods | $e_0^{\langle u_1 \rangle}$ ($y^+ \in [0,180]$) | $e_0^{\sqrt{\langle \tilde{u}_1^2 \rangle}}$ ($y^+ \in [30,180]$, inertial layer) |
|---|---|---|
| VMS-S (NO-SLIP BC) | 0.1141 | 0.2320 |
| VMS-S (WALL-LAW BC) | 0.1734 | 0.2094 |
| VMS-B (NO-SLIP BC) | 0.1786 | 0.3341 |
| SMA (NO-SLIP BC) | 0.1260 | 0.3123 |
| RB-VMS (Akkerman) | 0.2221 | 0.6104 |

To investigate more in detail statistical properties of this wall-bounded turbulence test, we plot second-order statistics as measure of turbulence intensities, by using either no-slip (for all methods) and wall-law (for VMS-S method) boundary conditions. Figure 2 displays the normalized (by the computed $u_\tau$) r.m.s. values of velocity fluctuations $\sqrt{\langle \tilde{u}_i^2 \rangle} = \left[ \langle u_i^2 \rangle - \langle u_i \rangle^2 \right]^{1/2}$ ($i = 1,2,3$) in wall coordinates $y^+$ at the upper half-width of the channel. If we compare with DNS data the various methods tested with no-slip boundary conditions, we can see slight differences for the curves associated to wall-normal and span-wise velocities, while the curve related to stream-wise velocity shows a noticeable over-prediction. We can also observe as for the r.m.s. values, the results obtained by the application of wall laws are only meaningful for the stream-wise component of the velocity, that is the leading one. Note that in this case the related curve starts at $y^+ = 11.5$, since the computational

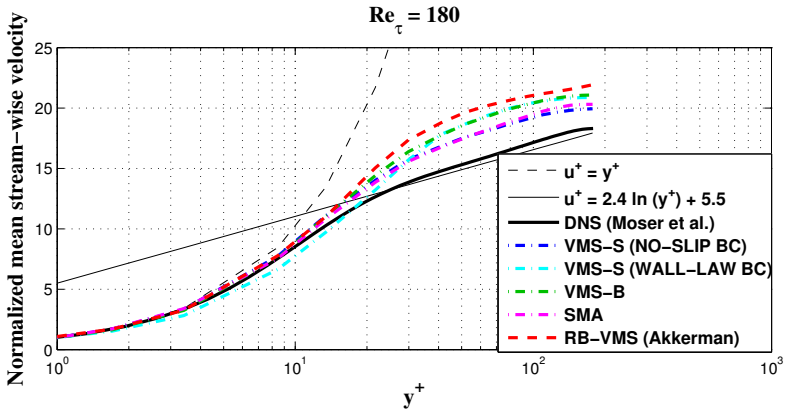


**Fig. 1**

Normalized mean stream-wise velocity profiles in wall coordinates $y^+$.

domain starts at $y^+ = 11.5$, and no extension is possible, as for the mean stream-wise velocity. However, a comparison with the other curves is possible starting from the first interior node at $y^+ \approx 30$, i.e. in the so-called *inertial layer*, as we could physically expect. Indeed, the inertial layer is where the logarithmic approximation of the friction-velocity $u^+$ is more accurate (see Figure 1). Actually, the best approximation of the r.m.s. stream-wise velocity fluctuation in the inertial layer is effectively given by the use VMS-S method with wall-laws, as shown quantitatively in Table 1 (second column), where the normalized discrete $L^2$-norm of the deviation from the DNS profile is computed, analogously to formula (43). Nevertheless, the results for the other "minor" velocity components are not acceptable compared with the DNS data at hand. In particular, this is true for the wall-normal component of the velocity, as in this case the model itself contemplates the imposition of a null wall-normal velocity at the fictitious boundary of the resulting reduced computational domain [see the boundary condition $\mathbf{u} \cdot \mathbf{n} = 0$ on $\Gamma_n$ in problem (1)], that is not expected by the use of standard no-slip boundary conditions.

Table 2 provides a quantitative picture for errors levels related to second-order statistics when the standard no-slip boundary conditions at the physical walls are incorporated in the various methods. Again, the VMS-S method is in general more in agreement with the DNS data, being SMA method the one that presents the largest distance from the experimental curves.

The numerical experiments confirm on one hand that the application of wall-law boundary conditions could provide (at least for the leading stream-wise component of the velocity) similar results to those obtained by the standard approach based on the use of no-slip boundary conditions, a refined mesh towards the walls and the Van Driest damping improvement, with a noticeable reduced computational cost. On another hand, they show that the VMS-S method gives quite good results for both first and second-order statistics (error levels similar to a more complex residual-based

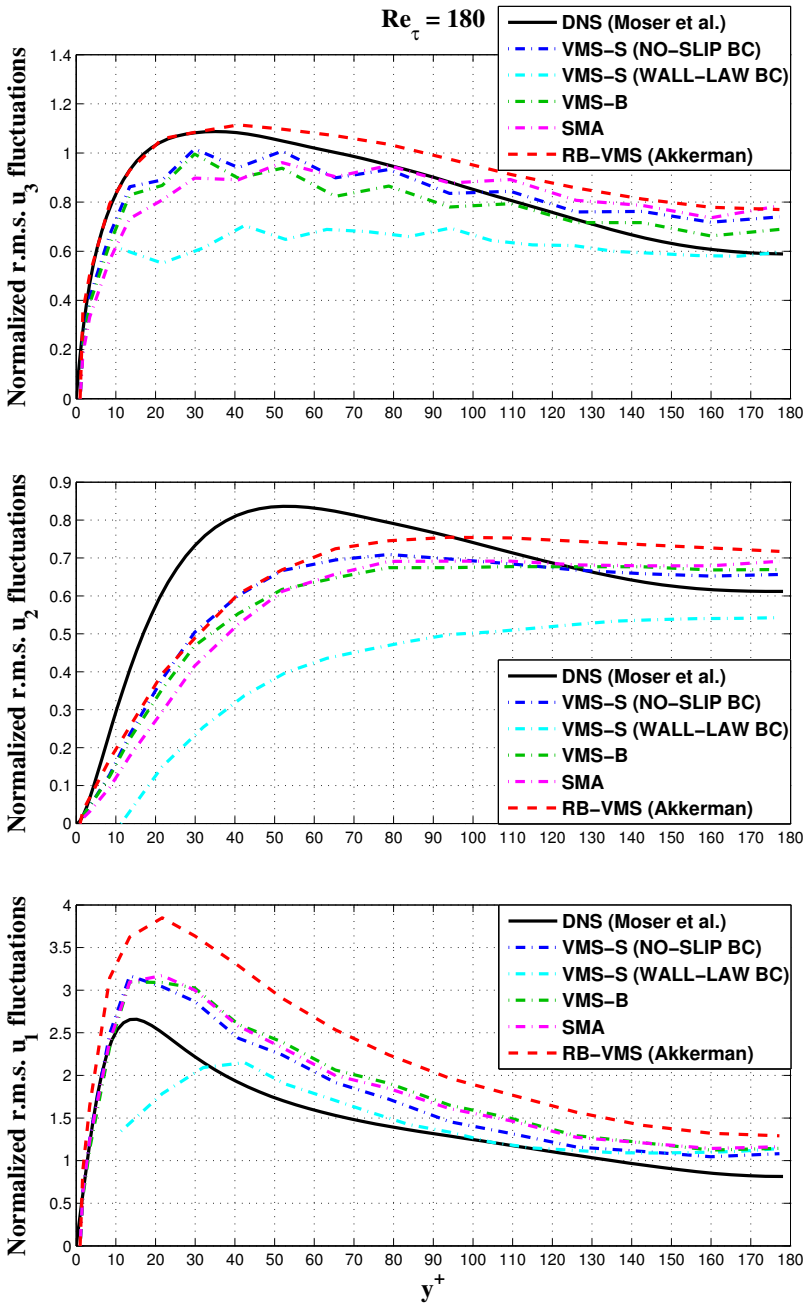


**Fig. 2**

Normalized r.m.s. velocity fluctuations profiles in wall coordinates $y^+$.

**Table 2** $L^2$-norm of the deviation from the DNS profiles for the second-order statistics.

| Methods | $e_0^{\sqrt{\langle \tilde{u}_1^2 \rangle}}$ | $e_0^{\sqrt{\langle \tilde{u}_2^2 \rangle}}$ | $e_0^{\sqrt{\langle \tilde{u}_3^2 \rangle}}$ |
|---|---|---|---|
| VMS-S (NO-SLIP BC) | 0.2252 | 0.1652 | 0.1108 |
| VMS-B (NO-SLIP BC) | 0.2881 | 0.2018 | 0.1246 |
| SMA (NO-SLIP BC) | 0.3002 | 0.2236 | 0.1597 |
| RB-VMS (Akkerman) | 0.5694 | 0.1753 | 0.1331 |

VMS method), in the worst condition of a very coarse basic discretization, thus providing a good compromise between accuracy and computational complexity, which is an important feature in the context of its practical performances.

**Acknowledgements** Research partially supported by the Spanish Government project MTM2012-36124-C02-01.

## References

1. N. Ahmed, T. Chacón Rebollo, V. John, and S. Rubino. Stability and error estimates of the fully discrete evolution NSE with LPS methods. Preprint, 2015.
2. I. Akkerman. *Adaptative variational multiscale formulations using the discrete Germano approach*. PhD thesis, Delft University of Technology, 2009.
3. Y. Bazilevs, V. M. Calo, J. A. Cottrell, T. J. R. Hughes, A. Reali, and G. Scovazzi. Variational multiscale residual-based turbulence modeling for large eddy simulation of incompressible flows. *Comput. Methods Appl. Mech. Engrg.*, 197(1-4):173–201, 2007.
4. Y. Bazilevs, C. Michler, V. M. Calo, and T. J. R. Hughes. Weak Dirichlet boundary conditions for wall-bounded turbulent flows. *Comput. Methods Appl. Mech. Engrg.*, 196(49-52):4853–4862, 2007.
5. Y. Bazilevs, C. Michler, V. M. Calo, and T. J. R. Hughes. Isogeometric variational multiscale modeling of wall-bounded turbulent flows with weakly enforced boundary conditions on unstretched meshes. *Comput. Methods Appl. Mech. Engrg.*, 199(13-16):780–790, 2010.
6. C. Bernardi, Y. Maday, and F. Rapetti. *Discrétisations variationnelles de problèmes aux limites elliptiques*, volume 45 of *Mathématiques & Applications*. Springer-Verlag, 2004.
7. L. C. Berselli, T. Iliescu, and W. J. Layton. *Mathematics of large eddy simulation of turbulent flows*. Scientific Computation. Springer-Verlag, Berlin, 2006.
8. T. Chacón Rebollo. An analysis technique for stabilized finite element solution of incompressible flows. *M2AN Math. Model. Numer. Anal.*, 35(1):57–89, 2001.
9. T. Chacón Rebollo, M. Gómez Mármol, V. Girault, and I. Sánchez Muñoz. A high order term-by-term stabilization solver for incompressible flow problems. *IMA J. Numer. Anal.*, 33(3):974–1007, 2013.
10. T. Chacón Rebollo, M. Gómez Mármol, and M. Restelli. Numerical analysis of penalty stabilized finite element discretizations of evolution Navier-Stokes equation. *J. Sci. Comput.*, 61(1):1–28, 2014.
11. T. Chacón Rebollo, M. Gómez Mármol, and S. Rubino. Derivation of the Smagorinsky model from a Galerkin discretization. In *Mascot11 Proc.*, volume 17 of *IMACS Series in Comp. and Appl. Math.*, pages 61–70, 2013.
12. T. Chacón Rebollo, M. Gómez Mármol, and S. Rubino. Numerical analysis of a finite element projection-based VMS turbulence model with wall laws. *Comput. Methods Appl. Mech. Engrg.*, 285:379–405, 2015.

13. T. Chacón Rebollo, F. Hecht, M. Gómez Mármol, G. Orzetti, and S. Rubino. Numerical approximation of the Smagorinsky turbulence model applied to the primitive equations of the ocean. *Math. Comput. Simulation*, 99:54–70, 2014.
14. T. Chacón Rebollo and R. Lewandowski. A variational finite element model for large-eddy simulations of turbulent flows. *Chin. Ann. Math. Ser. B*, 34(5):667–682, 2013.
15. T. Chacón Rebollo and R. Lewandowski. *Mathematical and numerical foundations of turbulence models and applications*. Birkhäuser, 2014.
16. H. Choi and P. Moin. Effects of the computational time step on numerical solutions of turbulent flow. *J. Comput. Phys.*, 113(1):1–4, 1994.
17. R. Codina. Comparison of some finite element methods for solving the diffusion-convection-reaction equation. *Comput. Methods Appl. Mech. Engrg.*, 156(1-4):185–210, 1998.
18. V. Gravemeier. Scale-separating operators for variational multiscale large eddy simulation of turbulent flows. *J. Comput. Phys.*, 212(2):400–435, 2006.
19. C. O. Horgan. Korn's inequalities and their applications in continuum mechanics. *SIAM Rev.*, 37(4):491–511, 1995.
20. T. J. R. Hughes, G. R. Feijóo, L. Mazzei, and J.-B. Quincy. The variational multiscale method—a paradigm for computational mechanics. *Comput. Methods Appl. Mech. Engrg.*, 166(1-2):3–24, 1998.
21. T. J. R. Hughes, L. Mazzei, and K. E. Jansen. Large eddy simulation and the variational multiscale method. *Comput. Vis. Sci.*, 3(1-2):47–59, 2000.
22. T. J. R. Hughes, L. Mazzei, A. A. Oberai, and A. Wray. The multiscale formulation of large eddy simulation: Decay of homogeneous isotropic turbulence. *Phys. Fluids*, 13(2):505–512, 2001.
23. T. J. R. Hughes, A. A. Oberai, and L. Mazzei. Large eddy simulation of turbulent channel flows by the variational multiscale method. *Phys. Fluids*, 13(6):1784–1799, 2001.
24. V. John, S. Kaya, and A. Kindl. Finite element error analysis for a projection-based variational multiscale method with nonlinear eddy viscosity. *J. Math. Anal. Appl.*, 344(2):627–641, 2008.
25. V. John and A. Kindl. Numerical studies of finite element variational multiscale methods for turbulent flow simulations. *Comput. Methods Appl. Mech. Engrg.*, 199(13-16):841–852, 2010.
26. W. P. Jones and M. Wille. Large eddy simulation of a jet in a cross-flow. In *10th Symposium on Turbulent Shear Flows*, volume 4, pages 1–6, 1995.
27. J. L. Lions. *Quelques méthodes de résolution des problèmes aux limites non linéaires*. Dunod, 2002.
28. R. Manning. On the flow of water in open channels and pipes. *Trans. Inst. Civil Eng. Ireland*, 20:161–207, 1891.
29. P. Moin and J. Kim. Numerical investigation of turbulent channel flow. *J. Fluid Mech.*, 118:341–377, 1982.
30. R. Moser, J. Kim, and N. N. Mansour. Direct numerical simulation of turbulent channel flow up to $Re_\tau = 590$. *Phys. Fluids*, 11(4):943–945, 1999.
31. C. Parés. Existence, uniqueness and regularity of solution of the equations of a turbulence model for incompressible fluids. *Appl. Anal.*, 43(3-4):245–296, 1992.
32. L. Prandtl. Über die ausgebildeten Turbulenz. *Zeitschrift für angewandte Mathematik und Mechanik*, 5:136–139, 1925.
33. S. Rubino. *Numerical modeling of turbulence by Richardson number-based and VMS models*. PhD thesis, Univeristy of Seville, 2014.
34. R. L. Scott and S. Zhang. Finite element interpolation of non-smooth functions satisfying boundary conditions. *Math. Comput.*, 54(190):483–493, 1990.
35. J. Simon. Compact sets in the space $L^p(0,T;B)$. *Ann. Mat. Pura Appl. (4)*, 146:65–96, 1987.
36. J. Smagorinsky. General circulation experiment with the primitive equations: I. The basic experiment. *Mon. Weather Rev.*, 91(3):99–164, 1963.
37. D. B. Spalding. A single formula for the "law of the wall". *J. Appl. Mech.*, 28(3):455–458, 1961.
38. E. R. Van Driest. On turbulent flow near a wall. *J. Aerosp. Sci.*, 23(11):1007–1011, 1956.
39. R. Verfürth. Finite element approximation of steady Navier-Stokes equations with mixed boundary conditions. *RAIRO Modél. Math. Anal. Numér.*, 19(3):461–475, 1985.

40. R. Verfürth. Finite element approximation of incompressible Navier-Stokes equations with slip boundary condition. *Numer. Math.*, 50(6):697–721, 1987.
41. T. Von Kármán. Mechanische Ähnlichkeit und Turbulenz. *Nachr. Ges. Wiss. Gottingen, Math. Phys. Klasse*, 58, 1930.